Precision Phenomenology at Colliders and Computational Methods

Gudrun Heinrich

KIT, Institute for Theoretical Physics (ITP)

Sommersemester 2021

version of May 31, 2021

Contents

Literature

- G. Dissertori, I. Knowles, M. Schmelling,
  Quantum Chromodynamics: High energy experiments and theory
  International Series of Monographs on Physics No. 115,
  Oxford University Press, Feb. 2003. Reprinted in 2005.

- R.K. Ellis, W.J. Stirling and B.R. Webber, *QCD and collider physics*,
  Cambridge University Press, Camb. Monogr. Part. Phys. Nucl. Phys.
  Cosmol. **8** (1996) 1.

- J. Campbell, J. Huston and F. Krauss,
  *The Black Book of Quantum Chromodynamics: A Primer for the LHC
  Era* Oxford University Press, December 2017.

- S. Dawson, C. Englert, T. Plehn,
  Higgs Physics: It ain't over till it's over, https://arxiv.org/abs/1808.01324;

- L. J. Dixon, *A brief introduction to modern amplitude methods*,
  https://arxiv.org/abs/1310.5353.

- G. Heinrich, *Collider Physics at the Precision Frontier*,
  https://arxiv.org/abs/2009.00516.

- V. A. Smirnov, *Analytic tools for Feynman integrals*, Springer Tracts
  Mod. Phys. **250** (2012) 1. doi:10.1007/978-3-642-34886-0.

1 Motivation: Collider Physics after the Higgs Discovery

2 A theoretical particle physicists' toolbox

2.1 Factorisation

2.2 Cross sections

2.3 Basics of QCD

2.3.1 Colour algebra

2.3.2 QCD Lagrangian

2.3.3 QCD Feynman rules

3 Example: top quark production

4 Higher orders in perturbation theory

4.1 Running coupling and scale dependence

In this section we would like to explain how it arises that theoretical predictions depend in general on at least one unphysical scale, the so-called *renormalisation scale* μ. In the case of hadronic initial state particles, there is also a *factorisation scale* μ_f involved. There can be even more unphysical scales, like fragmentation scales in the modelling of the fragmentation of final state particles into hadrons, parton shower matching scales, resummation scales, etc.

Let us first motivate how the dependence on a renormalisation scale arises. We mentioned already that the strong coupling, defined as $\alpha_s = g_s^2/(4\pi)$, is not really a constant. To leading order in the perturbative expansion, it obeys the relation

$$\alpha_s(Q^2) = \frac{1}{b_0 \log\left(Q^2/\Lambda_{QCD}^2\right)} \ , \tag{1}$$

where Λ_{QCD} is an energy scale below which non-perturbative effects start to dominate (the scale of bound states formation (hadrons)), and Q^2 is a larger energy scale, for example the centre-of-mass energy s of a scattering process. The coefficient b_0 is given by

$$b_0 = \frac{1}{4\pi}\left(\frac{11}{3}\,C_A - \frac{4}{3}T_R\,N_f\right) \ . \tag{2}$$

4

Note that $b_0 > 0$ for $N_f < 11/2\,C_A$.

Where does the running of the coupling come from? It is closely linked to renormalisation, which introduces the *renormalisation scale* μ.

Before we enter into the technicalities, let us look at a physical observable, for example the R-ratio which we encountered already,

$$R(s) = \frac{\sigma(e^+e^- \to \text{ hadrons})}{\sigma(e^+e^- \to \mu^+\mu^-)} \ . \tag{3}$$

We assume that the energy s exchanged in the scattering process is much larger than Λ_{QCD}.

At leading order in perturbation theory, we have to calculate tree-level diagrams for $e^+e^- \to f\bar{f}$, which however only represent a crude approximation. To get a more precise result, we should include quantum corrections, for example diagrams where virtual gluons are exchanged, such as the ones in Figs. 1a and 1b, where Fig. 1a shows corrections of order α_s and Fig. 1b shows example diagrams for $\mathcal{O}(\alpha_s^2)$ corrections. The perturbative expansion for R can be written as
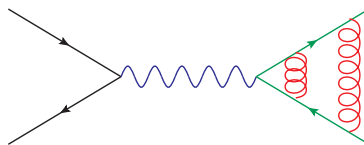
$$R(s) = K_{QCD}(s)\, R_0\ , \quad R_0 = N_c \sum_f Q_f^2\, \theta(s - 4m_f^2)\ ,$$

$$K_{QCD}(s) = 1 + \frac{\alpha_s(\mu^2)}{\pi} + \sum_{n \geq 2} C_n \left(\frac{s}{\mu^2}\right) \left(\frac{\alpha_s(\mu^2)}{\pi}\right)^n \ . \tag{4}$$

The higher the order in α_s the harder is the calculation. Meanwhile we know the C_n up to order α_s^4 [1,2].
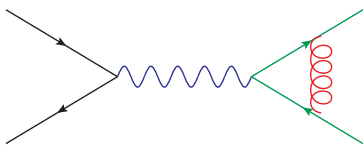
(a) 1-loop diagram contributing to $e^+e^- \to f\bar{f}$.

(b) 2-loop diagram example contributing to $e^+e^- \to f\bar{f}$.

However, if we try to calculate the loop diagrams, we will realize that some of the integrals over the loop momentum k are ill-defined. They diverge for $k \to \infty$. This is called an *ultraviolet divergence*. How to deal with them will be explained shortly. For the moment we just introduce an arbitrary cutoff

scale Λ_{UV} for the upper integration boundary. If we carried through the calculation, we would see that the dependence on the cutoff in diagram 1a cancels, which is a consequence of the Ward Identity in QED. However, if we go one order higher in α_s, calculating diagrams like the one in Fig. 1b, the cutoff-dependence does not cancel anymore. We obtain

$$K_{QCD}(s) = 1 + \frac{\alpha_s}{\pi} + \left(\frac{\alpha_s}{\pi}\right)^2 \left[c + b_0\pi \, \log \frac{\Lambda_{UV}^2}{s}\right] + \mathcal{O}(\alpha_s^3) \, . \qquad (5)$$

It looks like our result is infinite, as we should take the limit $\Lambda_{UV} \to \infty$. However, we did not claim that α_s is the coupling we measure. In fact, it is the "bare" coupling, also denoted as α_s^0, which appears in Eq. (5), and we can absorb the infinity in the bare coupling to arrive at the renormalised coupling, which is the one we measure.
In our case, this looks as follows. Define

$$\alpha_s(\mu) = \alpha_s^0 + b_0 \log \frac{\Lambda_{UV}^2}{\mu^2} \alpha_s^2 \, , \qquad (6)$$

then replace α_s^0 by $\alpha_s(\mu)$ and drop consistently all terms of order α_s^3. This leads to

$$K_{QCD}^{\mathrm{ren}}(\alpha_s(\mu), \mu^2/s) = 1 + \frac{\alpha_s(\mu)}{\pi} + \left(\frac{\alpha_s(\mu)}{\pi}\right)^2 \left[c + b_0\pi \, \log \frac{\mu^2}{s}\right] + \mathcal{O}(\alpha_s^3) \, . \quad (7)$$

K_{QCD}^{ren} is finite, but now it depends on the scale μ, both explicitly and through $\alpha_s(\mu)$. However, the hadronic R-ratio is a physical quantity and therefore cannot depend on the arbitrary scale μ. The dependence of K_{QCD} on μ is an artefact of the truncation of the perturbative series after the order α_s^2.

Renormalisation group and asymptotic freedom

Since the hadronic R-ratio $R^{\mathrm{ren}} = R_0 \, K_{QCD}^{\mathrm{ren}}$ cannot depend μ, we know

$$\mu^2 \frac{\mathrm{d}}{\mathrm{d}\mu^2} R^{\mathrm{ren}}(\alpha_s(\mu), \mu^2/Q^2) = 0 = \left(\mu^2 \frac{\partial}{\partial \mu^2} + \mu^2 \frac{\partial \alpha_s}{\partial \mu^2} \frac{\partial}{\partial \alpha_s}\right) R^{\mathrm{ren}}(\alpha_s(\mu), \mu^2/Q^2) \, .$$
$$(8)$$

Equation (8) is called *renormalisation group equation (RGE)*. Introducing the abbreviations

$$t = \ln \frac{Q^2}{\mu^2} \, , \qquad \beta(\alpha_s) = \mu^2 \frac{\partial \alpha_s}{\partial \mu^2} \, , \qquad (9)$$

6

the RGE becomes
$$\left(-\frac{\partial}{\partial t} + \beta(\alpha_s)\frac{\partial}{\partial \alpha_s}\right) R = 0 . \tag{10}$$

This first order partial differential equation can be solved by implicitly defining a function $\alpha_s(Q^2)$, the *running coupling*, by

$$t = \int_{\alpha_s}^{\alpha_s(Q^2)} \frac{\mathrm{d}x}{\beta(x)}, \quad \text{with} \quad \alpha_s \equiv \alpha_s(\mu^2) . \tag{11}$$

Differentiating Eq. (11) with respect to the variable t leads to

$$1 = \frac{1}{\beta(\alpha_s(Q^2))} \frac{\partial \alpha_s(Q^2)}{\partial t}, \quad \text{which implies} \quad \beta(\alpha_s(Q^2)) = \frac{\partial \alpha_s(Q^2)}{\partial t} .$$

The derivative of Eq. (11) with respect to α_s gives

$$0 = \frac{1}{\beta(\alpha_s(Q^2))} \frac{\partial \alpha_s(Q^2)}{\partial \alpha_s} - \frac{1}{\beta(\alpha_s)} \frac{\partial \alpha_s}{\partial \alpha_s} \Rightarrow \frac{\partial \alpha_s(Q^2)}{\partial \alpha_s} = \frac{\beta(\alpha_s(Q^2))}{\beta(\alpha_s)} . \tag{12}$$

It is now easy to prove that the value of R for $\mu^2 = Q^2$, $R(1, \alpha_s(Q^2))$, solves Eq. (10):

$$-\frac{\partial}{\partial t} R(1, \alpha_s(Q^2)) = -\frac{\partial R}{\partial \alpha_s(Q^2)} \frac{\partial \alpha_s(Q^2)}{\partial t} = -\beta(\alpha_s(Q^2)) \frac{\partial R}{\partial \alpha_s(Q^2)} \tag{13}$$

and

$$\beta(\alpha_s) \frac{\partial}{\partial \alpha_s} R(1, \alpha_s(Q^2)) = \beta(\alpha_s) \frac{\partial \alpha_s(Q^2)}{\partial \alpha_s} \frac{\partial R}{\partial \alpha_s(Q^2)} = \beta(\alpha_s(Q^2)) \frac{\partial R}{\partial \alpha_s(Q^2)} . \tag{14}$$

This means that the scale dependence in R enters only through $\alpha_s(Q^2)$, and that we can predict the scale dependence of R by solving Eq. (11), or equivalently,

$$\frac{\partial \alpha_s(Q^2)}{\partial t} = \beta\left(\alpha_s(Q^2)\right) . \tag{15}$$

We can solve Eq. (15) perturbatively using an expansion of the β-function

$$\beta(\alpha_s) = -b_0 \alpha_s^2 \left[1 + \sum_{n=1}^{\infty} b_n \, \alpha_s^n\right], \tag{16}$$

7

where $b_0 = \frac{\beta_0}{4\pi}$ and $b_0 b_1 = \frac{\beta_1}{(4\pi)^2}$, etc. Explicitly, up to NNLO:

$$\mu^2 \frac{\mathrm{d}\alpha_s(\mu)}{\mathrm{d}\mu^2} = -\alpha_s(\mu) \left[\beta_0 \left(\frac{\alpha_s(\mu)}{2\pi} \right) + \beta_1 \left(\frac{\alpha_s(\mu)}{2\pi} \right)^2 + \beta_2 \left(\frac{\alpha_s(\mu)}{2\pi} \right)^3 + \mathcal{O}(\alpha_s^4) \right] .$$

The first five coefficients are known [3], where the fifth one has been calculated only recently [4–8]. The first 3 coefficients ($\overline{\mathrm{MS}}$-scheme) are

$$\beta_0 = \frac{11\,C_A - 4T_R N_F}{6} ,$$

$$\beta_1 = \frac{17\,C_A^2 - 10 C_A T_R N_F - 6 C_F T_R N_F}{6} ,$$

$$\beta_2 = \frac{1}{432} \left(2857 C_A^3 + 108 C_F^2 T_R N_F - 1230 C_F C_A T_R N_F - 2830 C_A^2 T_R N_F \right.$$
$$\left. + 264 C_F T_R^2 N_F^2 + 316 C_A T_R^2 N_F^2 \right) . \tag{17}$$

Introducing Λ as integration constant with $L = \log(\mu^2/\Lambda^2)$ yields the following solution up to order NNLO:

$$\alpha_s(\mu) = \frac{4\pi}{\beta_0 L} \left(1 - \frac{\beta_1}{\beta_0^2} \frac{\log L}{L} + \frac{1}{\beta_0^2 L^2} \left(\frac{\beta_1^2}{\beta_0^2} \left(\log^2 L - \log L - 1 \right) + \frac{\beta_2}{\beta_0} \right) \right) . \tag{18}$$

Truncating the series Eq. (16) at leading order leads to the simple solution Eq. (1), or, without introducing Λ,

$$Q^2 \frac{\partial \alpha_s}{\partial Q^2} = \frac{\partial \alpha_s}{\partial t} = -b_0 \alpha_s^2 \Rightarrow -\frac{1}{\alpha_s(Q^2)} + \frac{1}{\alpha_s(\mu^2)} = -b_0\, t$$

$$\Rightarrow \alpha_s(Q^2) = \frac{\alpha_s(\mu^2)}{1 + b_0\, t\, \alpha_s(\mu^2)} . \tag{19}$$

Eq. (19) implies that

$$\alpha_s(Q^2) \xrightarrow{Q^2 \to \infty} \frac{1}{b_0 t} \xrightarrow{Q^2 \to \infty} 0 . \tag{20}$$

This behaviour is called *asymptotic freedom*: the larger Q^2, the smaller the coupling, so at very high energies (small distances), the quarks and gluons can be treated as if they were free particles. The behaviour of α_s as a function of Q^2 is illustrated in Fig. 2 including recent measurements. Note that the
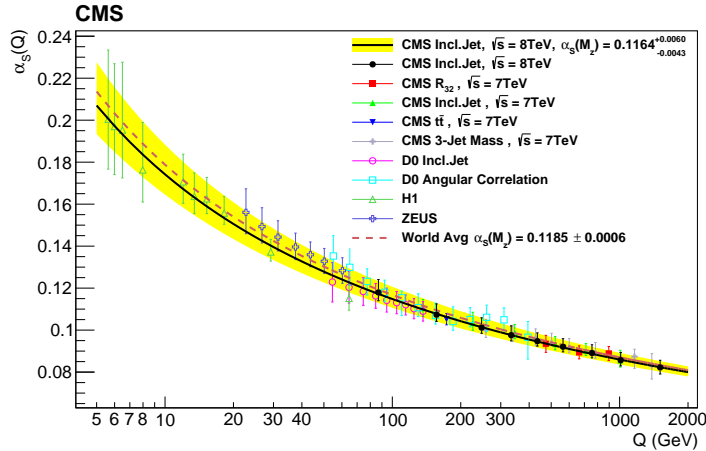
8

Figure 2: The running coupling $\alpha_s(Q^2)$. *Figure from arXiv:1609.05331.*

sign of b_0 is positive for QCD, while it is negative for QED. It can be proven that, in 4 space-time dimensions, only non-Abelian gauge theories can be asymptotically free. For the discovery of asymptotic freedom in QCD [9,10], Gross, Politzer and Wilczek got the Nobel Prize in 2004.

Note that in the derivation of the RGE above, we have assumed that the observable R does not depend on other mass scales like quark masses. However, the renormalisation group equations can be easily extended to include mass renormalisation, which will lead to running quark masses:

$$\left(\mu^2 \frac{\partial}{\partial \mu^2} + \beta(\alpha_s)\frac{\partial}{\partial \alpha_s} - \gamma_m(\alpha_s)m\frac{\partial}{\partial m}\right) R\left(\frac{Q^2}{\mu^2}, \alpha_s, \frac{m}{Q}\right) = 0 \, , \qquad (21)$$

where γ_m is called the *mass anomalous dimension* and the minus sign before γ_m is a convention. In a perturbative expansion we can write the mass anomalous dimension as $\gamma_m(\alpha_s) = c_0\,\alpha_s\left(1 + \sum_n c_n\alpha_s^n\right)$. The coefficients are known up to c_4 [11–14].

Scale uncertainties

From the perturbative solution of the RGE we can derive how a physical quantity $O^{(N)}(\mu)$, expanded in α_s as $O^{(N)}(\mu) = \sum_{n=0}^{N} C_n(\mu)\alpha_s^{n+k}(\mu^2)$ and truncated at order N in perturbation theory (k is the power of α_s at leading
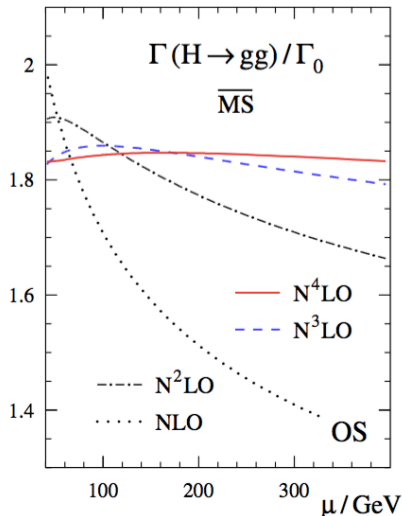
Figure 3: Example $H \to gg$ for the reduction of the scale dependence at higher orders. *Figure from Ref. [2], see also [8].*

order), changes with the renormalisation scale μ:

$$\frac{\mathrm{d}}{\mathrm{d}\log(\mu^2)}\, O^{(N)}(\mu) \sim \mathcal{O}\left(\alpha_s(\mu^2)^{N+1}\right) . \tag{22}$$

Therefore it is clear that, the more higher order coefficients c_n we can calculate, the less our result will depend on the unphysical scale μ^2. Therefore the dependence of the scale is used to estimate the uncertainty of a result calculated to a certain order in perturbation theory. Usually the scale is varied by a factor of two up and down. An example for the reduction of the scale dependence at higher orders is shown in Fig. 3.

An expansion up to NNLO of an observable O normalised to the LO cross section σ_0 can be written as

$$\frac{1}{\sigma_0}\frac{\mathrm{d}\sigma}{dO} \;=\; \left(\frac{\alpha_s}{2\pi}\right)\frac{\mathrm{d}C_1}{\mathrm{d}O} + \left(\frac{\alpha_s}{2\pi}\right)^2\frac{\mathrm{d}C_2}{\mathrm{d}O} + \left(\frac{\alpha_s}{2\pi}\right)^3\frac{\mathrm{d}C_3}{\mathrm{d}O} + \mathcal{O}(\alpha_s^4). \tag{23}$$

10

In terms of the running coupling $\alpha_s(\mu)$, the NNLO expression becomes

$$
\frac{1}{\sigma_0} \frac{\mathrm{d}\sigma}{\mathrm{d}O}(s, \mu^2, O) =
$$
$$
\left(\frac{\alpha_s(\mu)}{2\pi}\right) \frac{\mathrm{d}C_1}{\mathrm{d}O} + \left(\frac{\alpha_s(\mu)}{2\pi}\right)^2 \left(\frac{\mathrm{d}C_2}{\mathrm{d}O} + \frac{\mathrm{d}C_1}{\mathrm{d}O} \beta_0 \log \frac{\mu^2}{s}\right)
$$
$$
+ \left(\frac{\alpha_s(\mu)}{2\pi}\right)^3 \left(\frac{\mathrm{d}C_3}{\mathrm{d}O} + 2\frac{\mathrm{d}C_2}{\mathrm{d}O} \beta_0 \log \frac{\mu^2}{s} + \frac{\mathrm{d}C_1}{\mathrm{d}O} \left(\beta_0^2 \log^2 \frac{\mu^2}{s} + \beta_1 \log \frac{\mu^2}{s}\right)\right)
$$
$$
+ \mathcal{O}(\alpha_s^4) . \tag{24}
$$

As an example we consider an observable called *thrust*, shown in Fig. 4. Thrust is an example of so-called *event-shape* observables, which describes how "pencil-like" an event looks like. Events shapes can be defined based on hadronic tracks in the detector, avoiding jet definitions, and are particularly useful in e^+e^- annihilation, where the total energy of the partonic event is known. Thrust T is defined by

$$
T = \max_{\vec{n}} \frac{\sum_{i=1}^m |\vec{p}_i \cdot \vec{n}|}{\sum_{i=1}^m |\vec{p}_i|} , \tag{25}
$$

where $\vec{n}$ is a three-vector (the direction of the thrust axis) such that T is maximal. The particle three-momenta $\vec{p}_i$ are defined in the e^+e^- centre-of-mass frame.

Fig. 4 shows several features: 1. the scale dependence is reduced as the perturbative order increases, 2. the NNLO curve is closest to the data, 3. the data are still not well described by NNLO. The reasons for the latter are well understood: The perturbative prediction for the thrust distribution becomes singular as $T \to 1$, there is also a logarithmic divergence $\sim \ln(1-T)$. The latter is characteristic for events shape distributions. In perturbation theory at nth order logarithms of the form $\alpha_s^n \ln^m(1/(1-T))$ with $m \leq 2n$ appear. These spoil the convergence of the perturbative series and should be "resummed" if we want to make reliable prediction near the phase space region where $T \to 1$. Furthermore, the so-called *power corrections*, the terms of $\mathcal{O}\left(\frac{\Lambda}{Q}\right)^p$ in Eq. (??), play a role for this observable.

In hadronic collisions there is another scale, the factorisation scale μ_f, which needs to be taken into account when assessing the uncertainty of the theoretical prediction. Varying both μ_r and μ_f simultaneously in the same directions
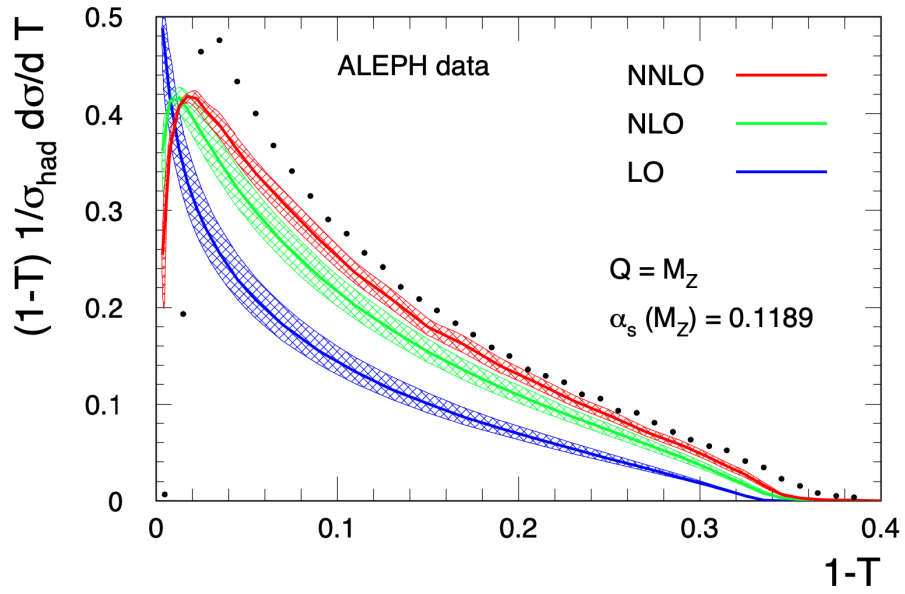
Figure 4: One minus thrust distribution at different orders in perturbation theory, including scale uncertainty bands. *Figure from Ref. [15].*

can lead to accidental cancellations and hence underestimation of the perturbative uncertainties. Therefore, in the presence of both μ_r and μ_f, often so-called *7-point scale variations* are performed, which means $\mu_{r,f} = c_{r,f}\mu_0$, where $c_r, c_f \in \{2, 1, 0.5\}$ and where the extreme variations $(c_r, c_f) = (2, 0.5)$ and $(c_r, c_f) = (0.5, 2)$ have been omitted.

Still, the question remains what to choose for the central scale μ_0. A convenient choice is a scale where the higher order corrections are small, i.e. a scale showing good "perturbative stability". In Fig. 3, a good choice would be $\mu_0 \approx 150\,\text{GeV}$.

Let us now see a few examples where such scale variations do not capture the true uncertainties. First some prelimiary remarks, along the lines of Ref. [16]. If there is only one scale μ_r involved, the the scale dependence of an observable is given through $\alpha_s(\mu_r)$, and we can use the beta-function, resp. Eq. (18), to move from a result at a scale μ_0 to a result at a different scale. For an observable O, known to order α_s^N,

$$O = \sum_{n=0}^{N} C_n(\mu_r) \alpha_s^{n+k}(\mu_r); ,$$

where k is the power of α_s at leading order, we therefore have (this time not normalised to the LO cross section)

$$O = C_0 \alpha_s^k(\mu_r) + \left(C_1 + b_0 C_0 \ln\left(\frac{\mu_r^2}{\mu_0^2}\right)\right) \alpha_s^{k+1}(\mu_r) + \mathcal{O}(\alpha_s^{k+2}) . \qquad (26)$$

Variations of μ_r will change the C_0-part of the $\mathcal{O}(\alpha_s^{k+2})$ term, however the magnitude of C_1 can only be known by direct calculation.

To illustrate the improvement in scale uncertainty that may occur at NNLO, let us consider the corrections up to (N)NLO for an observable as for example a jet cross section as a function of transverse energy, where $k = 2$. The renormalisation scale dependence is entirely predictable,

$$\begin{aligned}
\frac{d\sigma}{dE_T} = {} & \alpha_s^2(\mu_r) C_0 \\
& + \alpha_s^3(\mu_r) \left(C_1 + 2b_0 L C_0\right) \\
& + \alpha_s^4(\mu_r) \left(C_2 + 3b_0 L C_1 + (3b_0^2 L^2 + 2b_1 L) C_0\right) \qquad (27)
\end{aligned}$$

with $L = \ln(\mu_r/E_T)$. C_0 and C_1 are the known LO and NLO coefficients. Now assume that C_2 is an unknown NNLO term (note however that C_2 is

known meanwhile [17,18]). Fig. 5 shows that the scale dependence is systematically reduced by increasing the number of terms in the perturbative exp nsion. At NLO, there is always a turning point where the prediction is insensitive to small changes in μ_r. If this occurs at a scale far from the typically chosen values of μ_r, the NLO K-factor (defined as $K = 1 + \alpha_s(\mu_r)C_1/C_0$) will be large. At NNLO the scale dependence is clearly significantly reduced. However, a more quantitative statement requires knowledge of C_2.
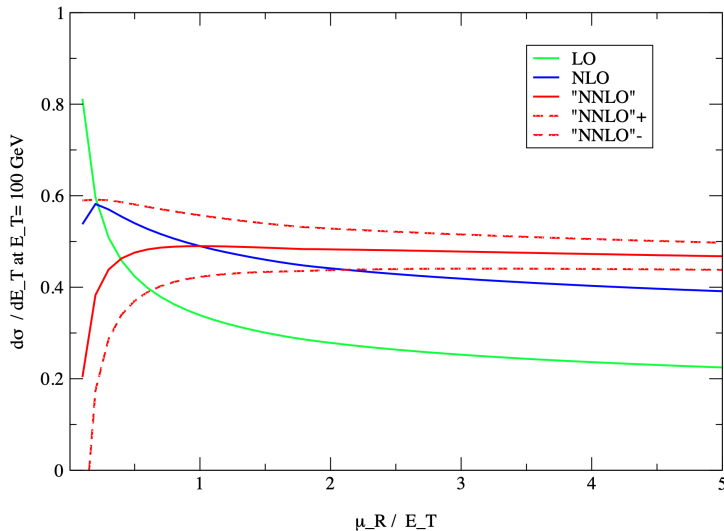

Figure 5: Single jet inclusive distribution at $E_T = 100$ GeV and $0.1 < |\eta| < 0.7$ at $\sqrt{s} = 1800$ GeV at LO (green), NLO (blue) and NNLO (red). The solid and dashed red lines show the NNLO prediction if $C_2 = 0$, $C_2 = \pm C_1^2/C_0$ respectively. Figure from Ref. [16].

For some processes, C_1 (and C_2) turned out to be pretty large, and the scale uncertainty bands obtained form 7-point scale variations do not (fully) overlap between the different orders. One such example is Higgs production in gluon fusion, known to order N^3LO. Fig. 6 shows a very nice stabilisation of the scale dependence, however the higher order corrections are very large. The standard scale uncertainty bands are shown in Fig. 7. Among the reasons for the large K-factors, in particular the NLO K-factor, are large colour factors and new partonic channels opening up.

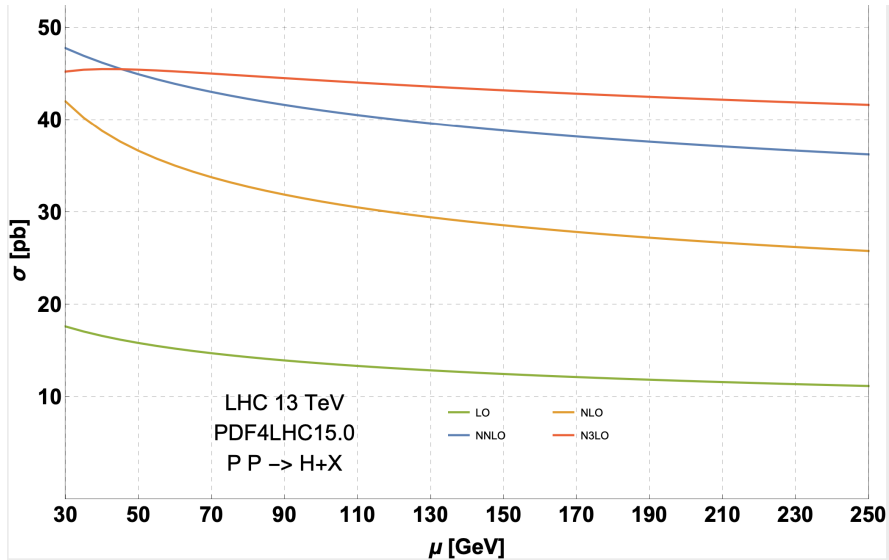In Fig. 8 the μ_f and μ_r dependence is shown separately. Usually one can see

Figure 6: Higgs production in gluon fusion, stabilisation of the scale dependence. Figure from Ref. [19].

that the perturbative series stabilises at latest between NNLO and N3LO. However, for charged current Drell-Yan production and a central scale of $Q = 100\,\mathrm{GeV}$, shown in Fig. 9, the NNLO and N3LO uncertainty bands do not overlap.

Looking at the μ_f dependence separately, one can see that the NNLO band is accidentally small, see Fig. 10.

Furthermore, the behaviour of the scale uncertainty bands can depend sensitively on the definition of the central scale, see Fig. 11. The different central scale choices are

- the individual jet transverse momentum p_T. This however can lead to the scale being set to values that are not representative of the scale of the underlying hard scattering process.

- The leading-jet transverse momentum $p_{T,1}$, This scale uses the transverse momentum of the hardest jet in the event, which is a better proxy for the scale of the hard interaction compared to the $\mu = p_T$ choice.

- The scalar sum of the transverse momenta of all reconstructed jets H_T, $H_T = \sum_{i\in\mathrm{jets}} p_{T,i}$.
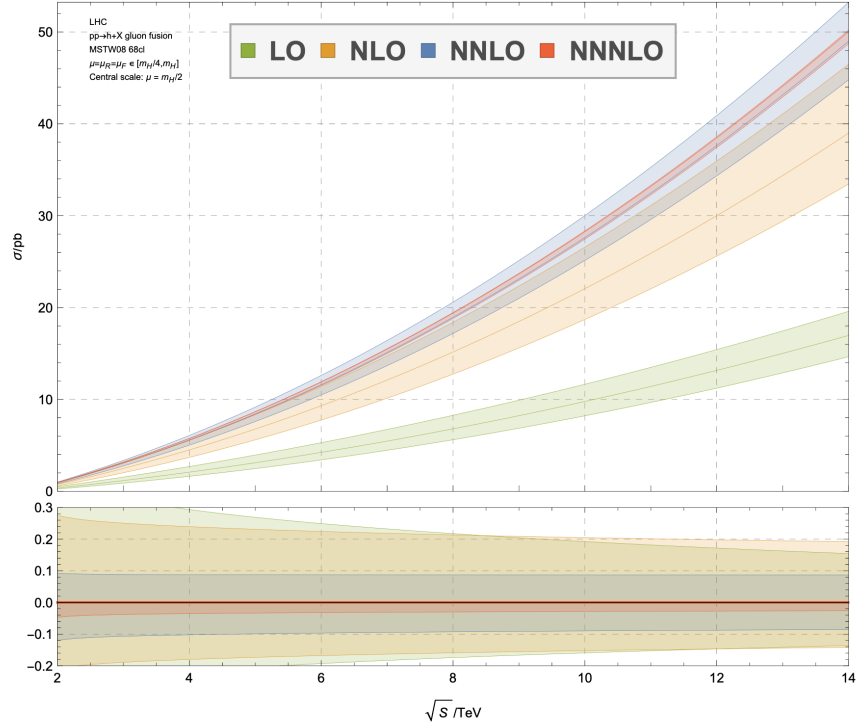
15

Figure 7: Scale uncertainty bands for Higgs production in gluon fusion. Figure from Ref. [20].

- The scalar sum of the transverse momenta of all partons $\hat{H}_T$: the transverse momentum sum is not based on the reconstructed jets, but instead obtained as the transverse momentum sum of all partons in the event: $\hat{H}_T = \sum_{i \in \text{partons}} p_{T,i}$. This scale choice also has the advantage of being insensitive to the jet reconstruction applied in the analysis and is an infrared-safe event shape variable.
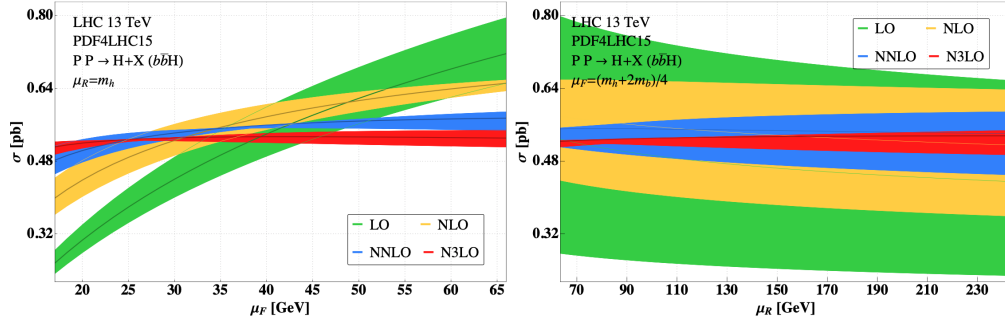
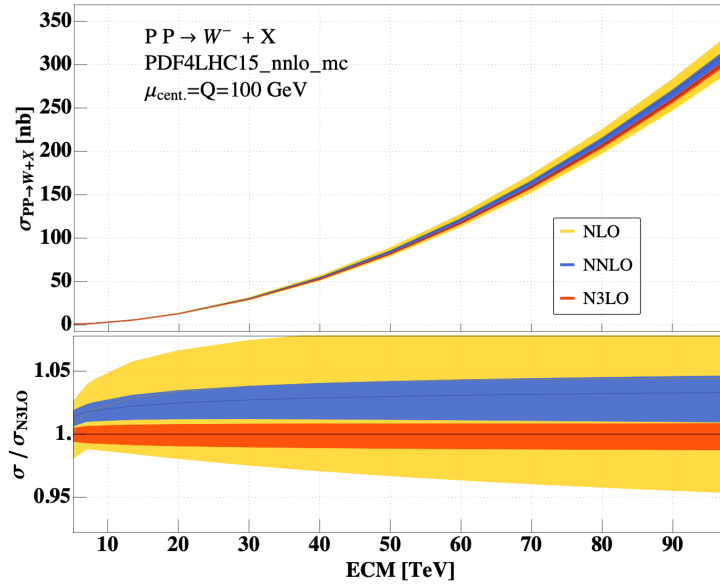Figure 8: Higgs production in bottom quark fusion. Figure from Ref. [21].

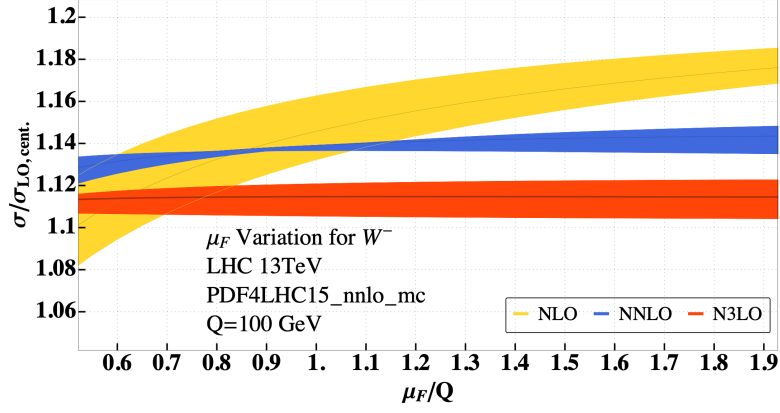Figure 9: Charged current Drell-Yan production, $pp \to W^-$. Figure from Ref. [22].

Figure 10: Charged current Drell-Yan production, μ_f-dependence. Figure from Ref. [22].
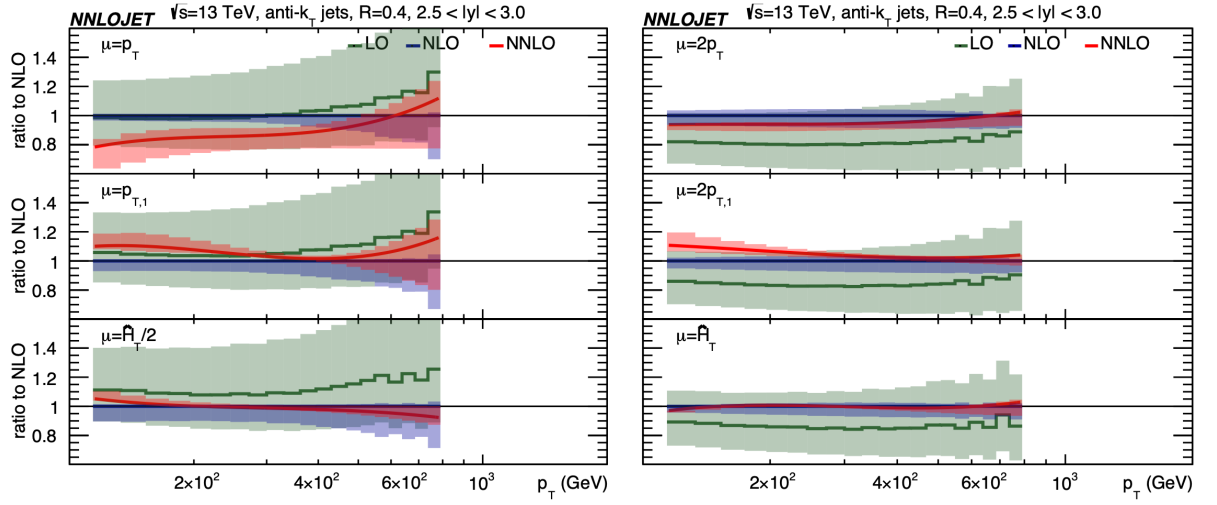

Figure 11: Inclusive jet p_T spectrum integrated over rapidity at LO (green), NLO (blue) and NNLO (red) normalised to the NLO prediction as a function of the central scale choice for cone size $R = 0.4$. Figure from Ref. [23].

4.2 Loops and divergences

4.3 Dimensional regularisation

Tree level results in QCD are mostly not accurate enough to match the current experimental precision and suffer from large scale uncertainties. When calculating higher orders, we encounter singularities: ultraviolet (UV) singularities, and infrared (IR) singularities due to soft or collinear massless particles. Therefore the introduction of a *regulator* is necessary.

Let us first have a look at UV singularities: The expression for the one-loop two-point function shown below naively would be
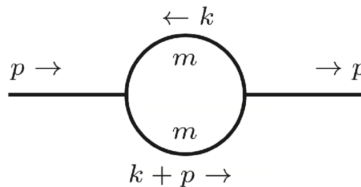

Figure 12: One-loop two-point function ("bubble").

$$I_2 = \int_{-\infty}^{\infty} \frac{d^4 k}{(2\pi)^4} \frac{1}{[k^2 - m^2 + i\delta][(k+p)^2 - m^2 + i\delta]} \ . \tag{28}$$

If we are only interested in the behaviour of the integral for $|k| \to \infty$ we can neglect the masses, transform to polar coordinates and obtain

$$I_2 \sim \int d\Omega_3 \int_0^{\infty} d|k| \frac{|k|^3}{|k|^4} \ . \tag{29}$$

This integral is clearly not well-defined. If we introduce an upper cutoff Λ (and a lower limit $|k|_{\min}$ because we neglected the masses and p^2, which would serve as an IR regulator), it is regulated:

$$I_2 \sim \int_{|k|_{\min}}^{\Lambda} d|k| \frac{1}{|k|} \sim \log\left(\frac{\Lambda}{|k|_{\min}}\right) \ . \tag{30}$$

The integral has a logarithmic UV divergence for $\Lambda \to \infty$. The problem with cut-off regularisation with a regulator Λ is that it is neither a Lorentz invariant nor a gauge invariant way to regulate integrals over loop momenta.

A regularisation method which preserves the symmetries is *dimensional regularisation.*

Dimensional regularisation has been introduced in 1972 by 't Hooft and Veltman [24] (and by Bollini and Giambiagi [25]) as a method to regularise UV divergences in a gauge invariant way, thus completing the proof of renormalisability.

The idea is to work in $D = 4 - 2\epsilon$ space-time dimensions. Divergences for $D \to 4$ will appear as poles in $1/\epsilon$. This means that the Lorentz algebra objects (momenta, polarisation vectors, metric tensor) live in a D-dimensional space. The γ-algebra also has to be extended to D dimensions. How to treat internal and external Lorentz vectors and the γ-algebra is not unique. There are several *regularisation schemes* within dimensional regularisation. For example, when doing a calculation in supersymmetry, you may not want to use a scheme where massless bosons have $D - 2$ polarisation states while massless fermions have 2 polarisation states. Of course the different schemes must lead to the same result for physical quantities.

An important feature of dimensional regularisation is that it regulates IR singularities, i.e. divergences occurring when massless particles become soft and/or collinear, as well. Ultraviolet divergences occur for loop momenta $k \to \infty$, so in general the UV behaviour becomes better for $\epsilon > 0$, while the IR behaviour becomes better for $\epsilon < 0$. Certainly we cannot have $D < 4$ and $D > 4$ at the same time. What is formally done is to first assume the IR divergences are regulated in some other way, e.g. by assuming all external legs are off-shell or by introducing a small mass for all massless particles. In this case all poles in $1/\epsilon$ will be of UV nature and renormalisation can be performed. Then we can analytically continue to the whole complex D-plane, in particular to $\mathrm{Re}(D) > 4$. If we now remove the auxiliary IR regulator, the IR divergences will show up as $1/\epsilon$ poles. (This is however not done in practice, where all poles just show up as $1/\epsilon$ poles, and after UV renormalisation, the remaining poles must be of IR nature.)

Naive degree of divergence

The naive degree of UV divergence ω of an integral can be determined by power counting: if we work in D dimensions at L loops, and consider an integral with P propagators and n_l factors of the loop momentum belonging to loop $l \in \{1, \ldots, L\}$ in the numerator, we have $\omega = D\,L - 2P + 2\sum_l \lfloor n_l/2 \rfloor$, where $\lfloor n_l/2 \rfloor$ is the nearest integer less or equal to $n_l/2$. We have logarith-

mic, linear, quadratic,... overall divergences for $\omega = 0, 1, 2, \ldots$ and no UV divergence for $\omega < 0$. This means that in 4 dimensions at one loop, we have UV divergences in all two-point functions, three-point functions with rank ≥ 2 and four-point functions with rank ≥ 4.

These considerations do not take into account UV subdivergences of multi-loop integrals, or a reduction of the degree of divergence due to gauge cancellations. Therefore ω is called *naive* or *superficial* degree of divergence.

In dimensional regularisation, the only change to the Feynman rules to be made is to multiply the couplings in the Lagrangian by a factor μ^ϵ: $g \to g\mu^\epsilon$, where μ is an arbitrary mass scale. This ensures that each term in the Lagrangian has the correct mass dimension. The momentum integration involves $\int \frac{d^D k}{(2\pi)^D}$ for each loop.

4.4 One-loop integrals

Integration in D dimensions

We first consider a scalar one-loop diagram with N external legs and N propagators, as gien in (31). The case with loop momenta in the numerator ("tensor integrals") will be treated later. If k is the loop momentum, the momenta of the propagators are $q_a = k + r_a$, where $r_a = \sum_{i=1}^{a} p_i$. If we define all momenta as incoming, momentum conservation implies $\sum_{i=1}^{N} p_i = 0$ and hence $r_N = 0$.
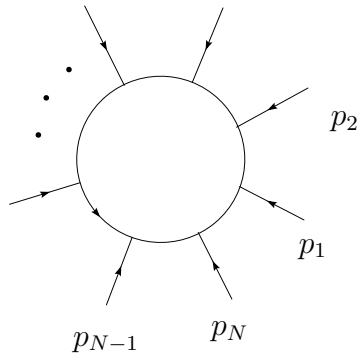

Figure 13: Generic one-loop integral

$$I_N^D = \int_{-\infty}^{\infty} \frac{d^D k}{i\pi^{\frac{D}{2}}} \frac{1}{\prod_{i=1}^{N}(q_i^2 - m_i^2 + i\delta)} \ . \tag{31}$$

We use the integration measure $d^D k / i\pi^{\frac{D}{2}} \equiv d\kappa$ to avoid ubiquitous factors of $i\pi^{\frac{D}{2}}$ which will arise upon momentum integration.

Feynman parameters

To combine products of denominators of the type $d_i^{n_i} = [(k+r_i)^2 - m_i^2 + i\delta]^{n_i}$ into one single denominator, we can use the identity

$$\frac{1}{d_1^{n_1} d_2^{n_2} \ldots d_N^{n_N}} = \frac{\Gamma(\sum_{i=1}^{N} n_i)}{\prod_{i=1}^{N} \Gamma(n_i)} \int_0^{\infty} \prod_{i=1}^{N} dz_i \, z_i^{n_i-1} \frac{\delta(1 - \sum_{j=1}^{N} z_j)}{[z_1 d_1 + z_2 d_2 + \ldots + z_N d_N]^{\sum_{i=1}^{N} n_i}}$$
$$\tag{32}$$

The integration parameters z_i are called *Feynman parameters*. For generic one-loop diagrams we have $n_i = 1 \, \forall i$. Propagator powers n_i different from one become important when we derive relations between integrals.

Schwinger parametrisation

An alternative to Feynman parametrisation is the so-called "Schwinger parametrisation", based on

$$\frac{1}{d_i^{n_i}} = \frac{1}{\Gamma(n_i)} \int_0^{\infty} d\alpha \, \alpha^{n_i-1} \exp(-\alpha \, d_i), \quad Re(d_i) > 0 \ , \tag{33}$$

which can be derived from the definition of the Γ-function

$$\Gamma(t) = \int_0^{\infty} dx \, x^{t-1} \exp(-x), \quad Re(t) > 0 \ . \tag{34}$$

The Gaussian integration formula

$$\int_{-\infty}^{\infty} d^D r_E \exp(-\alpha \, r_E^2) = \left(\frac{\pi}{\alpha}\right)^{\frac{D}{2}} \ , \quad \alpha > 0 \tag{35}$$

can be used to integrate over the momenta (after Wick rotation) in the Schwinger parametrisation.

Simple example: one-loop two-point function

For $N = 2$, (2-point integral), the Feynman parametrisation is given by

$$
\begin{aligned}
I_2 &= \int_{-\infty}^{\infty} d\kappa \, \frac{1}{[k^2 - m^2 + i\delta][(k+p)^2 - m^2 + i\delta]} \\
&= \Gamma(2) \int_0^{\infty} dz_1 dz_2 \int_{-\infty}^{\infty} d\kappa \, \frac{\delta(1 - z_1 - z_2)}{[z_1 (k^2 - m^2) + z_2 ((k+p)^2 - m^2) + i\delta]^2} \\
&= \int_0^1 dx \int_{-\infty}^{\infty} d\kappa \, \frac{1}{[k^2 + 2xk \cdot p + xp^2 - m^2 + i\delta]^2} \, ,
\end{aligned}
\tag{36}
$$

where we have substituted $z_1 = (1 - x) \, u, z_2 = x$ before the last line. As the momentum integral is shift invariant, we can substitute $l = k + xp$ to eliminate the term linear in the loop momentum, to arrive at

$$
I_2 = \int_0^1 dx \int_{-\infty}^{\infty} \frac{\mathrm{d}^D l}{i\pi^{\frac{D}{2}}} \, \frac{1}{[l^2 + p^2 x(1 - x) - m^2 + i\delta]^2} \, .
\tag{37}
$$

For integrals with more external legs the linear term can be eliminated by an analogous shift of the loop momentum. Therefore, the generic form of a one-loop integral after Feynman parametrisation and after having performed the shift to achieve a quadratic form in the loop momentum is given by

$$
I_N^D = \Gamma(N) \int_0^{\infty} \prod_{i=1}^N dz_i \, \delta(1 - \sum_{j=1}^N z_j) \int_{-\infty}^{\infty} \frac{\mathrm{d}^D l}{i\pi^{\frac{D}{2}}} \, \left[l^2 - R^2 + i\delta \right]^{-N}
\tag{38}
$$

where for $N = 2$ and both propagators massive we have just derived $R = -p^2 x(1 - x) + m^2$.

For the general case, one finds

$$
R^2 = -\frac{1}{2} \sum_{i,j=1}^N z_i \, z_j \, \mathcal{S}_{ij} \qquad \text{with}
\tag{39}
$$

$$
\mathcal{S}_{ij} = (r_i - r_j)^2 - m_i^2 - m_j^2 \, , \quad \sum_{i=1}^N z_i = 1 \, .
\tag{40}
$$

The matrix $\mathcal{S}_{ij}$, sometimes also called *Cayley matrix*, is the quantity encoding all the kinematic dependence of the integral. It plays a major role in the algebraic reduction of tensor integrals or integrals with higher N to simpler objects, as well as in the analysis of the kinematic singularities of the integrand.
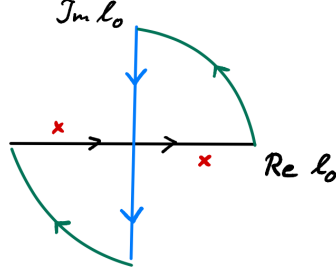
Figure 14: Integration contour after Wick rotation.

Momentum integration for scalar one-loop N-point integrals

Now we perform the momentum integration for an integral of the form Eq. (38). Remember that we are in Minkowski space, where $l^2 = l_0^2 - \vec{l}^2$, so temporal and spatial components are not on equal footing. The poles of the denominator in Eq. (38) are located at $l_0^2 = R^2 + \vec{l}^2 - i\delta \Rightarrow l_0^{\pm} \simeq \pm\sqrt{R^2 + \vec{l}^2} \mp i\,\delta$. Thus the $i\delta$ term shifts the poles away from the real axis in the l_0-plane.

For the integration over the loop momentum, we better work in Euclidean space where $l_E^2 = \sum_{i=1}^{D} l_i^2$. Hence we make the transformation $l_0 \to i\,l_4$, such that $l^2 \to -l_E^2 = l_4^2 + \vec{l}^2$, which implies that the integration contour in the complex l_0-plane is rotated by $90°$ such that the contour in the complex l_4-plane looks as shown below. This is called *Wick rotation*. We see that the $i\delta$ prescription is exactly such that the contour does not enclose any poles. Therefore the integral over the closed contour is zero, and we can use the identity

$$\int\limits_{-\infty}^{\infty} dl_0 f(l_0) = i \int\limits_{-\infty}^{\infty} dl_4 f(l_4) \tag{41}$$

Our integral now reads

$$I_N^D = (-1)^N \Gamma(N) \int_0^\infty \prod_{i=1}^{N} dz_i\, \delta(1 - \sum_{l=1}^{N} z_l) \int_{-\infty}^{\infty} \frac{d^D l_E}{\pi^{\frac{D}{2}}}\, \left[l_E^2 + R^2 - i\delta\right]^{-N} \tag{42}$$

Now we can introduce polar coordinates in D dimensions to evaluate the

momentum integral.

$$\int_{-\infty}^{\infty} d^D l_E = \int_0^{\infty} dr\, r^{D-1} \int d\Omega_{D-1} \; , \; r = \sqrt{l_E^2} = \left(\sum_{i=1}^4 l_i^2 \right)^{\frac{1}{2}} \quad (43)$$

$$\int d\Omega_{D-1} = V(D) = \frac{2\pi^{\frac{D}{2}}}{\Gamma(\frac{D}{2})} \quad (44)$$

where $V(D)$ is the volume of a unit sphere in D dimensions, which we encountered already in the context of D-dimensional phase space integrals. Thus we have

$$I_N^D = 2(-1)^N \frac{\Gamma(N)}{\Gamma(\frac{D}{2})} \int_0^{\infty} \prod_{i=1}^N dz_i\, \delta(1 - \sum_{l=1}^N z_l) \int_0^{\infty} dr\, r^{D-1} \frac{1}{[r^2 + R^2 - i\delta]^N}$$

Substituting $r^2 = x$:

$$\int_0^{\infty} dr\, r^{D-1} \frac{1}{[r^2 + R^2 - i\delta]^N} = \frac{1}{2} \int_0^{\infty} dx\, x^{D/2-1} \frac{1}{[x + R^2 - i\delta]^N} \quad (45)$$

Now the substitution $x = zR^2$ can be done to arrive at

$$\frac{1}{2} \int_0^{\infty} dx\, x^{D/2-1} \frac{1}{[x + R^2 - i\delta]^N} = \frac{1}{2} \left[R^2 - i\delta \right]^{\frac{D}{2} - N} \int_0^{\infty} dz\, z^{D/2-1} \left[1 + z \right]^{-N} . \quad (46)$$

Note that we still carry along the $-i\delta$ term because it can be useful to indicate the direction of the analytic continuation when performing the integrals over the Feynman parameters. As it only indicates an infinitesimal shift, we can always rescale δ by a positive quantity. The z-integral can be identified as the Euler Beta-function $B(a, b)$, defined as

$$B(a, b) = \int_0^{\infty} dz\, \frac{z^{a-1}}{(1 + z)^{a+b}} = \int_0^1 dy\, y^{a-1}(1 - y)^{b-1} = \frac{\Gamma(a)\Gamma(b)}{\Gamma(a + b)} \; , \quad (47)$$

to finally arrive at

$$I_N^D = (-1)^N \Gamma(N - \frac{D}{2}) \int_0^{\infty} \prod_{i=1}^N dz_i\, \delta(1 - \sum_{l=1}^N z_l) \left[R^2 - i\delta \right]^{\frac{D}{2} - N} . \quad (48)$$

The integration over the Feynman parameters remains to be done, but for one-loop applications, the integrals we need to know explicitly have maximally $N = 4$ external legs. Integrals with $N > 4$ can be expressed in terms

25

of boxes, triangles, bubbles and tadpoles (in the case of massive propagators). The analytic expressions for these "master integrals" are well-known. The most complicated analytic functions which can appear at one loop are dilogarithms.

The generic form of the derivation above makes clear that we do not have to go through the procedure of Wick rotation explicitly each time. All we need (for scalar integrals) is to use the following general formula for D-dimensional momentum integration (in Minkowski space, and after having performed the shift to have a quadratic form in the denominator):

$$\int \frac{d^D l}{i\pi^{\frac{D}{2}}} \frac{(l^2)^r}{[l^2 - R^2 + i\delta]^N} = (-1)^{N+r} \frac{\Gamma(r + \frac{D}{2})\Gamma(N - r - \frac{D}{2})}{\Gamma(\frac{D}{2})\Gamma(N)} \left[R^2 - i\delta\right]^{r - N + \frac{D}{2}}$$

$$(49)$$

Example one-loop two-point function

Applying the above procedure to our two-point function, we obtain

$$I_2 = \Gamma(2 - \frac{D}{2}) \int_0^1 dx \left[-p^2 x (1-x) + m^2 - i\delta\right]^{\frac{D}{2} - 2}. \qquad (50)$$

For $m^2 = 0$, the result can be expressed in terms of Γ-functions:

$$I_2 = \left(-p^2\right)^{\frac{D}{2} - 2} \Gamma(2 - D/2) B(D/2 - 1, D/2 - 1), \qquad (51)$$

where the $B(a, b)$ is defined in Eq. (47). The two-point function has an UV pole which is contained in

$$\Gamma(2 - D/2) = \Gamma(\epsilon) = \frac{1}{\epsilon} - \gamma_E + \mathcal{O}(\epsilon), \qquad (52)$$

where γ_E is "Euler's constant", $\gamma_E = \lim_{n \to \infty} \left(\sum_{j=1}^{n} \frac{1}{j} - \ln n\right) = 0.5772156649\ldots$.

Including the factor $g^2 \mu^{2\epsilon}$ which usually comes with the loop, and multiplying by $\frac{i\pi^{\frac{D}{2}}}{(2\pi)^D}$ for the normalisation conventions, we obtain

$$g^2 \mu^{2\epsilon} \frac{i\pi^{\frac{D}{2}}}{(2\pi)^D} I_2 = (4\pi)^\epsilon i \frac{g^2}{(4\pi)^2} \Gamma(\epsilon) \left(-p^2/\mu^2\right)^{-\epsilon} B(1 - \epsilon, 1 - \epsilon). \qquad (53)$$

Remarks:

- As the combination $\Delta = \frac{1}{\epsilon} - \gamma_E + \ln(4\pi)$ always occurs in combination with a pole, in the so-called $\overline{\text{MS}}$ subtraction scheme ("modified Minimal Subtraction"), the whole combination Δ is subtracted in the renormalisation procedure.

- Scaleless integrals (i.e. integrals containing no dimensionful scale like masses or external momenta) are zero in dimensional regularisation, we use

$$\int_{-\infty}^{\infty} \frac{d^D k}{k^{2\rho}} = 0 \ . \tag{54}$$

Tensor integrals

If we have loop momenta in the numerator, the integration procedure is essentially the same, except for combinatorics and additional Feynman parameters in the numerator. The substitution $k = l - Q$ introduces terms of the form $(l - Q)^{\mu_1} \ldots (l - Q)^{\mu_r}$ into the numerator of eq. (38). As the denominator is symmetric under $l \to -l$, only the terms with even numbers of l^μ in the numerator will give a non-vanishing contribution upon l-integration. We can use a *form factor representation* of a tensor integral, where the Lorentz structure has been extracted, each Lorentz tensor multiplying a scalar quantity, the *form factor*.

Historically, tensor integrals occurring in one-loop amplitudes were reduced to scalar integrals using so-called *Passarino-Veltman* reduction [26]. It is based on the fact that at one loop, scalar products of loop momenta with external momenta can always be expressed as combinations of propagators. The problem with Passarino-Veltman reduction is that it introduces powers of inverse Gram determinants $1/(\det G)^r$ for the reduction of a rank r tensor integral. This can lead to numerical instabilities upon phase space integration in kinematic regions where $\det G \to 0$.

Example for *Passarino-Veltman reduction:*
Consider the form factor representation of a rank one three-point integral

$$
\begin{aligned}
I_3^{D,\mu} &= \int_{-\infty}^{\infty} d\kappa \, \frac{k^\mu}{[k^2 + i\delta][(k+p_1)^2 + i\delta][(k+p_1+p_2)^2 + i\delta]} = A_1 \, r_1^\mu + A_2 \, r_2^\mu \\
r_1 &= p_1 \ , \ r_2 = p_1 + p_2 \ .
\end{aligned}
$$

27

Contracting with r_1 and r_2 and using the identities

$$k \cdot r_i = \frac{1}{2} \left[(k+r_i)^2 - k^2 - r_i^2 \right] \ , \ i \in \{1,2\}$$

we obtain, after cancellation of numerators

$$\begin{pmatrix} 2\,r_1 \cdot r_1 & 2\,r_1 \cdot r_2 \\ 2\,r_2 \cdot r_1 & 2\,r_2 \cdot r_2 \end{pmatrix} \begin{pmatrix} A_1 \\ A_2 \end{pmatrix} = \begin{pmatrix} R_1 \\ R_2 \end{pmatrix} \tag{55}$$

$$R_1 = I_2^D(r_2) - I_2^D(r_2 - r_1) - r_1^2 I_3(r_1, r_2)$$
$$R_2 = I_2^D(r_1) - I_2^D(r_2 - r_1) - r_2^2 I_3(r_1, r_2) \ .$$

Solving for the form factors A_1 and A_2 we see that the solution involves the inverse of the Gram matrix $G_{ij} = 2\,r_i \cdot r_j$.

Libraries where the scalar integrals and tensor one-loop form factors can be obtained numerically:

- `LoopTools` [27, 28]

- `OneLoop` [29]

- `golem95` [30–32]

- `Collier` [33]

- `Package-X` [34]

Scalar integrals only: `QCDLoop` [35, 36].

The calculation of one-loop amplitudes with many external legs is most efficiently done using "unitarity-cut-inspired" methods, for a review see e.g. Ref. [37]. One of the advantages is that it allows (numerical) reduction at *integrand level* (rather than integral level), which helps to avoid the generation of spurious terms which can blow up intermediate expressions.

5   Example: Higgs production

References

[1] P. A. Baikov, K. G. Chetyrkin, J. H. Kühn and J. Rittinger, *Complete $\mathcal{O}(\alpha_s^4)$ QCD Corrections to Hadronic Z-Decays*, *Phys. Rev. Lett.* **108** (2012) 222003, [`1201.5804`].

[2] F. Herzog, B. Ruijl, T. Ueda, J. A. M. Vermaseren and A. Vogt, *On Higgs decays to hadrons and the R-ratio at N^4LO*, *JHEP* **08** (2017) 113, [`1707.01044`].

[3] T. van Ritbergen, J. A. M. Vermaseren and S. A. Larin, *The Four loop beta function in quantum chromodynamics*, *Phys. Lett.* **B400** (1997) 379–384, [`hep-ph/9701390`].

[4] P. A. Baikov, K. G. Chetyrkin and J. H. Kühn, *Five-Loop Running of the QCD coupling constant*, *Phys. Rev. Lett.* **118** (2017) 082002, [`1606.08659`].

[5] F. Herzog, B. Ruijl, T. Ueda, J. A. M. Vermaseren and A. Vogt, *The five-loop beta function of Yang-Mills theory with fermions*, *JHEP* **02** (2017) 090, [`1701.01404`].

[6] T. Luthe, A. Maier, P. Marquard and Y. Schröder, *The five-loop Beta function for a general gauge group and anomalous dimensions beyond Feynman gauge*, *JHEP* **10** (2017) 166, [`1709.07718`].

[7] K. G. Chetyrkin, G. Falcioni, F. Herzog and J. A. M. Vermaseren, *Five-loop renormalisation of QCD in covariant gauges*, *JHEP* **10** (2017) 179, [`1709.08541`].

[8] J. Davies, M. Steinhauser and D. Wellmann, *Completing the hadronic Higgs boson decay at order α_s^4*, *Nucl. Phys.* **B920** (2017) 20–31, [`1703.02988`].

[9] D. J. Gross and F. Wilczek, *Ultraviolet Behavior of Nonabelian Gauge Theories*, *Phys. Rev. Lett.* **30** (1973) 1343–1346.

[10] H. D. Politzer, *Reliable Perturbative Results for Strong Interactions?*, *Phys. Rev. Lett.* **30** (1973) 1346–1349.

[11] P. A. Baikov, K. G. Chetyrkin and J. H. Kühn, *Quark Mass and Field Anomalous Dimensions to $\mathcal{O}(\alpha_s^5)$*, *JHEP* **10** (2014) 076, [1402.6611].

[12] P. A. Baikov, K. G. Chetyrkin and J. H. Kühn, *Five-loop fermion anomalous dimension for a general gauge group from four-loop massless propagators*, *JHEP* **04** (2017) 119, [1702.01458].

[13] A. G. Grozin, P. Marquard, A. V. Smirnov, V. A. Smirnov and M. Steinhauser, *Matching the heavy-quark fields in QCD and HQET at four loops*, *Phys. Rev. D* **102** (2020) 054008, [2005.14047].

[14] F. Herren and A. E. Thomsen, *On Ambiguities and Divergences in Perturbative Renormalization Group Functions*, 2104.07037.

[15] A. Gehrmann-De Ridder, T. Gehrmann, E. W. N. Glover and G. Heinrich, *NNLO corrections to event shapes in e+ e- annihilation*, *JHEP* **12** (2007) 094, [0711.4711].

[16] E. W. N. Glover, *Progress in NNLO calculations for scattering processes*, *Nucl. Phys. B Proc. Suppl.* **116** (2003) 3–7, [hep-ph/0211412].

[17] J. Currie, E. W. N. Glover and J. Pires, *Next-to-Next-to Leading Order QCD Predictions for Single Jet Inclusive Production at the LHC*, *Phys. Rev. Lett.* **118** (2017) 072002, [1611.01460].

[18] M. Czakon, A. van Hameren, A. Mitov and R. Poncelet, *Single-jet inclusive rates with exact color at $\mathcal{O}\ (\alpha_s^4)$*, *JHEP* **10** (2019) 262, [1907.12911].

[19] B. Mistlberger, *Higgs boson production at hadron colliders at N^3LO in QCD*, *JHEP* **05** (2018) 028, [1802.00833].

[20] C. Anastasiou, C. Duhr, F. Dulat, F. Herzog and B. Mistlberger, *Higgs Boson Gluon-Fusion Production in QCD at Three Loops*, *Phys. Rev. Lett.* **114** (2015) 212001, [1503.06056].

[21] C. Duhr, F. Dulat, V. Hirschi and B. Mistlberger, *Higgs production in bottom quark fusion: matching the 4- and 5-flavour schemes to third order in the strong coupling*, JHEP **08** (2020) 017, [2004.04752].

[22] C. Duhr, F. Dulat and B. Mistlberger, *Charged current Drell-Yan production at N^3LO*, JHEP **11** (2020) 143, [2007.13313].

[23] J. Currie, A. Gehrmann-De Ridder, T. Gehrmann, E. W. N. Glover, A. Huss and J. a. Pires, *Infrared sensitivity of single jet inclusive production at hadron colliders*, JHEP **10** (2018) 155, [1807.03692].

[24] G. 't Hooft and M. J. G. Veltman, *Regularization and Renormalization of Gauge Fields*, Nucl. Phys. **B44** (1972) 189–213.

[25] C. G. Bollini and J. J. Giambiagi, *Dimensional Renormalization: The Number of Dimensions as a Regularizing Parameter*, Nuovo Cim. **B12** (1972) 20–26.

[26] G. Passarino and M. J. G. Veltman, *One Loop Corrections for e+ e- Annihilation Into mu+ mu- in the Weinberg Model*, Nucl. Phys. **B160** (1979) 151–207.

[27] T. Hahn, *Feynman Diagram Calculations with FeynArts, FormCalc, and LoopTools*, PoS **ACAT2010** (2010) 078, [1006.2231].

[28] T. Hahn and M. Perez-Victoria, *Automatized one loop calculations in four-dimensions and D-dimensions*, Comput. Phys. Commun. **118** (1999) 153–165, [hep-ph/9807565].

[29] A. van Hameren, *OneLOop: For the evaluation of one-loop scalar functions*, Comput. Phys. Commun. **182** (2011) 2427–2438, [1007.4716].

[30] J. P. Guillet, G. Heinrich and J. F. von Soden-Fraunhofen, *Tools for NLO automation: extension of the golem95C integral library*, Comput. Phys. Commun. **185** (2014) 1828–1834, [1312.3887].

[31] G. Cullen, J. P. Guillet, G. Heinrich, T. Kleinschmidt, E. Pilon, T. Reiter et al., *Golem95C: A library for one-loop integrals with complex masses*, Comput. Phys. Commun. **182** (2011) 2276–2284, [1101.5595].

[32] T. Binoth, J. P. Guillet, G. Heinrich, E. Pilon and T. Reiter, *Golem95: A Numerical program to calculate one-loop tensor integrals with up to six external legs*, Comput. Phys. Commun. **180** (2009) 2317–2330, [0810.0992].

[33] A. Denner, S. Dittmaier and L. Hofer, *Collier: a fortran-based Complex One-Loop LIbrary in Extended Regularizations*, Comput. Phys. Commun. **212** (2017) 220–238, [1604.06792].

[34] H. H. Patel, *Package-X: A Mathematica package for the analytic calculation of one-loop integrals*, Comput. Phys. Commun. **197** (2015) 276–290, [1503.01469].

[35] S. Carrazza, R. K. Ellis and G. Zanderighi, *QCDLoop: a comprehensive framework for one-loop scalar integrals*, Comput. Phys. Commun. **209** (2016) 134–143, [1605.03181].

[36] R. K. Ellis and G. Zanderighi, *Scalar one-loop integrals for QCD*, JHEP **02** (2008) 002, [0712.1851].

[37] R. Ellis, Z. Kunszt, K. Melnikov and G. Zanderighi, *One-loop calculations in quantum field theory: from Feynman diagrams to unitarity cuts*, Phys. Rept. **518** (2012) 141–250, [1105.4319].